Finite Element Evaluation of Bearing Instrumentation Method

J. Austin, Dr. David Talbot, Dr. Donald Houser and Dr. Sandeep M. Vijayakar

This paper presents an evaluation of measurements being taken on a 750 kW wind turbine gearbox being tested by the National Renewable Energy Laboratory (NREL). High-speed stage gears and bearings have been identified as critical components of the gearbox; during gearbox testing, these components were instrumented and tests were developed to evaluate loads on high-speed tapered roller bearings (TRBs). In this paper an advanced finite element-based contact modeling procedure has been applied to model the high-speed stage with the bearings fully modeled in order to evaluate strain levels. A major conclusion is that the strains of the slotted grooves are at such a level that they have acceptable signal-to-noise levels. This was verified by the results of the initial experiments presented here.

Introduction

Motivation and gearbox configuration. The National Renewable Energy Laboratory (NREL) has made a commitment to address wind turbine gearbox reliability as part of its research agenda. A gearbox reliability collaborative (GRC) was developed to address major gearbox issues with the goal of increasing the overall reliability of wind turbines. Many gearbox problems may be a result of poor communication and feedback during the design, operation, and maintenance of turbines (Ref. 1). The GRC is aimed at uniting these equally critical elements of the design process and encouraging collaboration and information sharing. A 750 kW turbine design, representative of many turbines currently in service, was selected by a committee of experts and gearbox consultants hired by NREL under the GRC.

The majority of observed failures appears to initiate at bearing locations, and are not a result of gear failures or gear-tooth design deficiencies. The failures appear to initiate at bearing locations and then propagate into other components of the gearbox. During the first iteration of testing there were a number of component failures seen in the gearbox, many of which were attributed to lubricant starvation. Components damaged in this gearbox included the high-speed gearset, sun spline, and planet bearings (Ref. 2). The gearbox underwent a redesign and so began a new iteration of testing.

The GRC gearbox is shown in Figure 1; its design is a speed increaser that includes a planetary stage followed by two parallel shaft stages. The gearbox has a power capacity of 750 kW, with an

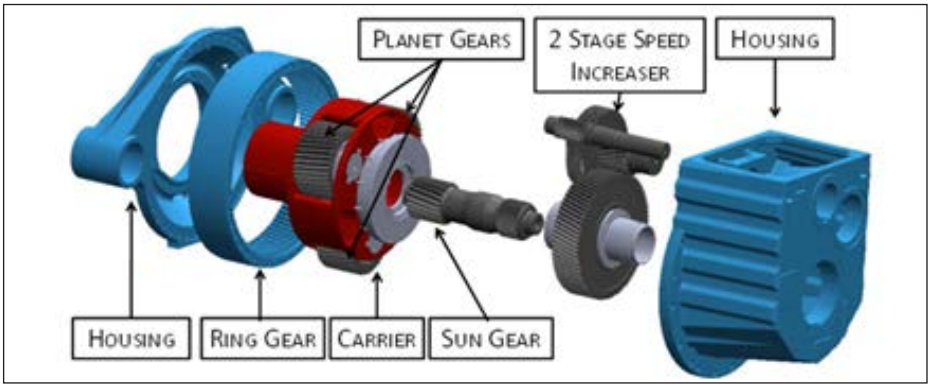

Figure 1 Exploded view of example gearbox (Ref. 3).

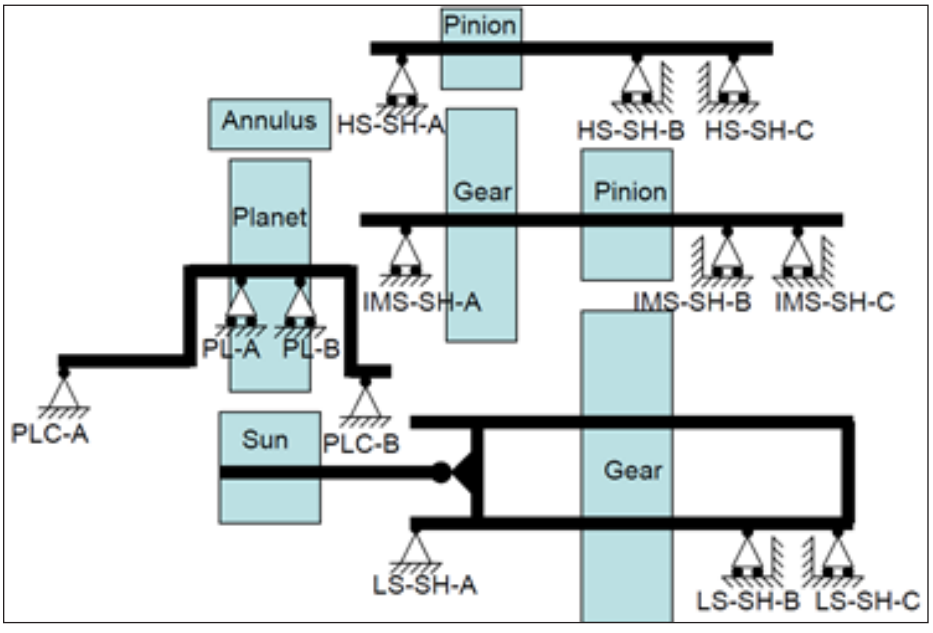

Figure 2 Gearbox bearing locations and nomenclature (Ref. 3).

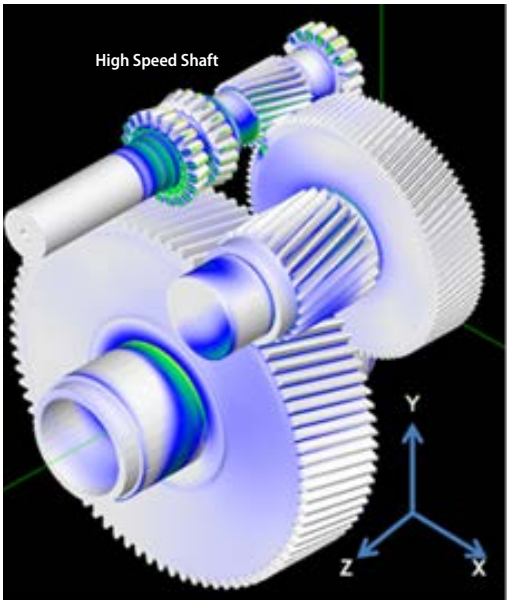

Figure 3 ***Transmission3D*** **model showing high-speed, intermediate speed, and low- speed shaft stages.**

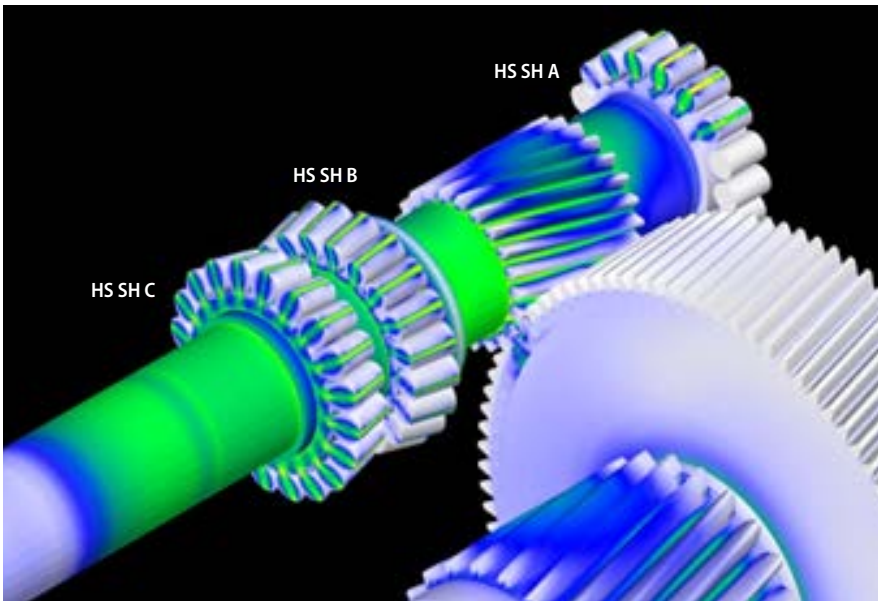

Figure 4 ***Transmission3D*** **high-speed shaft stage with bearings fully modeled.**

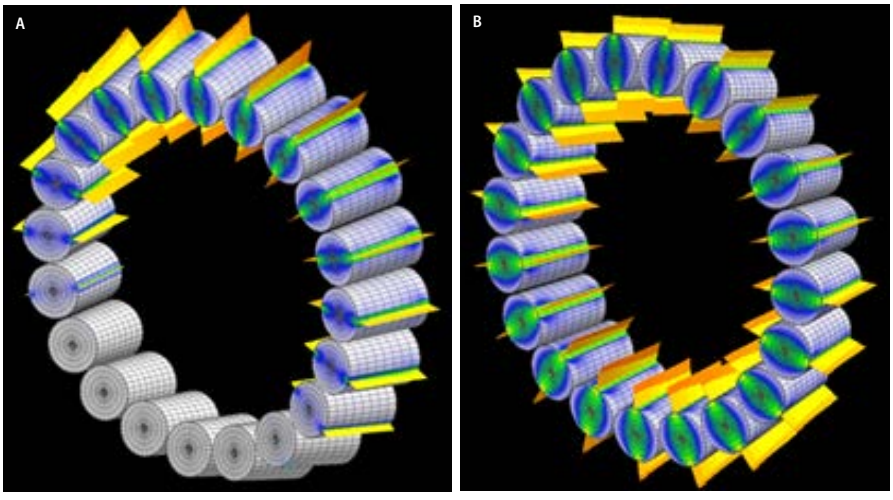

Figure 5 **A) HS SH B and B) HS SH C roller contact pressure distribution.**

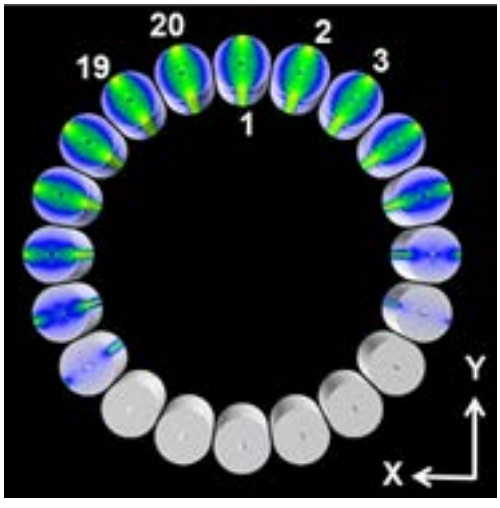

Figure 6 **HS SH B TRB rollers with numbering convention.**

overall speed increase ratio of 1:81.491. The nominal input speed is 22 rpm, with the output speed at 1,800 rpm. A 323 kN-m input torque is required on the rotor blades to operate the generator at full-rated power.

The following nomenclature will be used throughout the rest of this document when referencing internal components of the gearbox:

"***Upwind components***" are those located on the entrance side of the stage before power has passed through the gear.

These may also be termed "***rotor side***," as they are located closer to the rotor.

"Downwind components" are those located on the aft end of the shaft.

Parallel shaft stages are comprised of three separate shafts — each supported by three bearings. The bearing configuration of each shaft consists of a cylindrical roller bearing on the upwind portion of the shaft: (LS-SH-A, IMS-SH-A, HS-SH-A); and a pair of tapered roller bearings (TRBs): (LS-SH-B, IMS-SH-B, HS-SH-B, LS-SH-C, IMS-SH-C, HS-SH-C) on the downwind portion of the shaft. Bearing locations and naming convention are shown (Fig. 2). The subject of this paper will be the high-speed pinion shaft bearings (HS-SH-B, HS-SH-C) that support the upper shaft of Figure 2.

Transmission3D and Calyx. *Transmission3D* is a linear, finite element (FE) contact analysis program developed by Advanced Numerical Solutions LLC (Ref. 4), specifically designed for the analysis of multi-mesh-geared drivetrains. The program empowers the user to model the housing, bearings, shafts, planet carrier, and gears as deformable bodies. Gear microgeometries can be included, as well as assembly and manufacturing errors. Bearings are generated similar to gears, and can include crowning on the rollers and races, as well as clearance and preload.

The greatest benefit of *Transmission3D* is in the contact algorithm. Gear, bearing, and spline stresses are localized and influenced by microgeometries on the micron scale. *Transmission3D* uses a unique contact analysis solver — *Calyx* — that utilizes a hybrid algorithm of finite elements to predict far field displacements, and an elastic half-space model to predict relative displacements local to the contact region

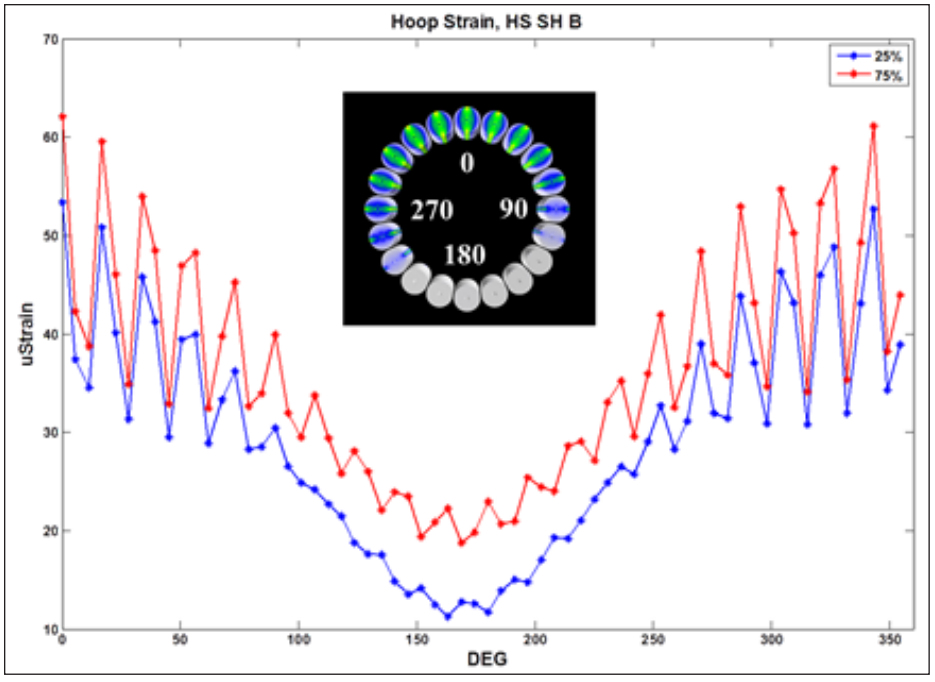

Figure 7 Unmodified outer raceway hoop strain of HS SH B for one-time step.

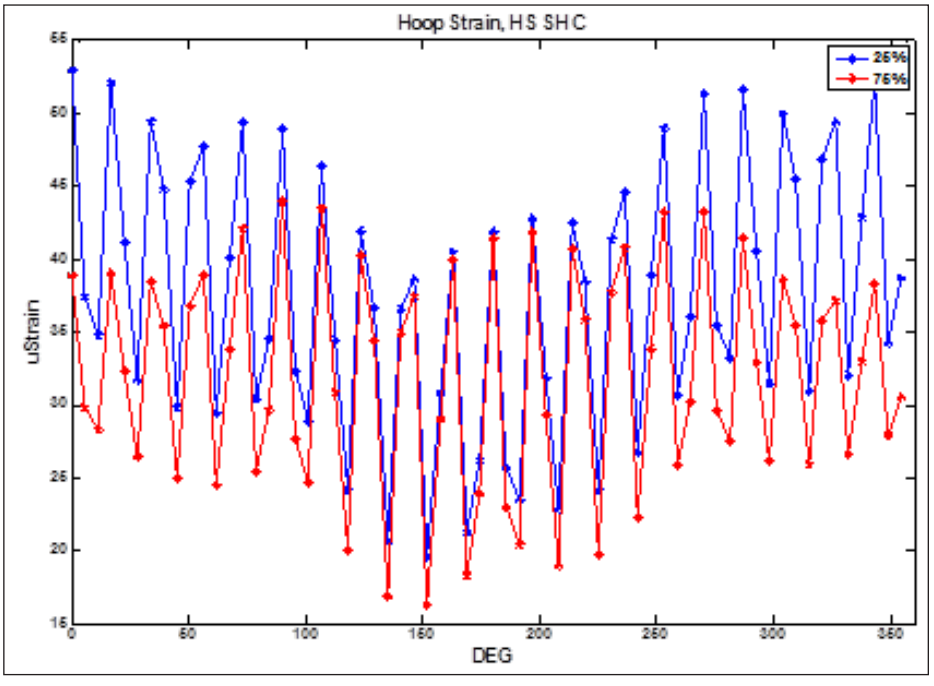

Figure 8 Unmodified outer raceway hoop strain of HS SH C for one-time step.

Table 1 Simulated peak-to-peak strains at groove locations with and without the modified bearing race.

Location	HS SH B (micro-strain)				HS SH C (micro-strain)			
	No Groove		With Groove		No Groove		With Groove	
	25%	75%	25%	75%	25%	75%	25%	75%
A	19	23	133	150	18	11	103	81
B	3	10	47	5	21	19	134	163
C	2	4	-14	17	19	21	153	107
D	7	13	107	100	19	15	154	135

(Ref. 5). But in doing so, *Calyx* does not require a highly refined FE mesh.

High-Speed Shaft Analysis

The high-speed stage gears and bearings are acknowledged to be critical components of the gearbox (Refs. 1–2); there previously had been very little instrumentation of the high-speed shaft, gears, and bearings. During the next phase of testing, this portion of the gearbox was to be instrumented. In this next phase, tests were developed to evaluate the loads on the TRBs (Ref. 6). Gauges were placed in axial grooves machined into the outer race of the TRBs. Each bearing has four axial grooves, with two-gages-per-groove.

There was initial concern as to whether the strain levels would be high enough in the bearing raceways to provide an adequate signal-to-noise ratio. The outer race of the bearing is tapered; the groove geometry was tapered as well, with the intent of maintaining a constant radial thickness of the raceway along the groove.

In this analysis, contact was included in the model at all gear mesh locations and at the high-speed bearings; all other bearings were included as stiffness matrices. The high-speed, intermediate-speed, and low-speed stages are shown in Figure 3. The fully modeled bearings can also be seen, and are shown in detail in Figure 4, which also displays the naming convention.

Model parameters. An analysis was completed with and without the modified race under 100% torque loading conditions. The TRBs were preloaded with 70 micron of negative clearance to accommodate mounting preload and loads due to thermal expansion of the bearing components. The cylindrical roller bearing HS SH A includes 18 micron of diametric clearance. In this opposing TRB configuration, bearing HS SH C will carry the thrust load generated at the high-speed gear mesh, adding to the initial preload of that bearing and relieving the preload from HS SH B. Figure 5 shows the contact pressure distributions on a) HS SH B and b) HS SH C. It can be seen that all of the rollers in HS SH C are in contact; as mentioned previously, this bearing carries the thrust force generated at the gear mesh,

which keeps all rollers under load. HS SH B however, has approximately 30% of the rollers out of contact.

Bearing strain results. Figure 6 displays the numbering convention used for both TRBs. The first roller in each bearing is located at zero degrees — or top-dead-center (TDC) of the bearing — and increases clockwise while looking downwind (from the left, Fig. 2). The hoop strain was extracted around the circumference of the outer raceway (Figs. 7– 8). The strain was sampled at two axial locations, i.e. — at 25% and 75% of the axial length of the raceway. The results of this analysis are from one time step and can be viewed as if the race was unwrapped and laid flat on the page. Roller 1 is at TDC (0 degrees). The peaks correspond to roller positions; a peak indicates that a roller was directly under that location and a valley indicates that two rollers are straddling that point. The race with grooves has locations at 0° (Groove A); 90° (Groove B); 180° (Groove C); and 270° (Groove D). Differences in load distribution along the rollers themselves should result in shifts in strain values between the two axial locations, and could be used as an indication of roller load distribution. Figures 9 and 10 illustrate the strains extracted around the circumference of the outer race with the machined grooves; the groove locations are labeled. Table 1 shows the peak-to-peak, predicted strain indicating the strain caused by direct application of load by a passing roller.

Discussion

The grooves, as indicated in Figures 7-10, increased the simulated bearing race strains by as much as 300 %. HS SH B had two groove locations that were either very lightly loaded or were outside the load zone completely — i.e., locations b and c — respectively. These locations did not see the same amplification as those located directly in the bearing load zone. In general the groove geometry increased strains by a considerable amount. One detriment to modifying the bearing outer race may be that the roller-to-roller load distribution could be affected by the modification. Figures 11 and 12 show the predicted roller loads of HS SH B and

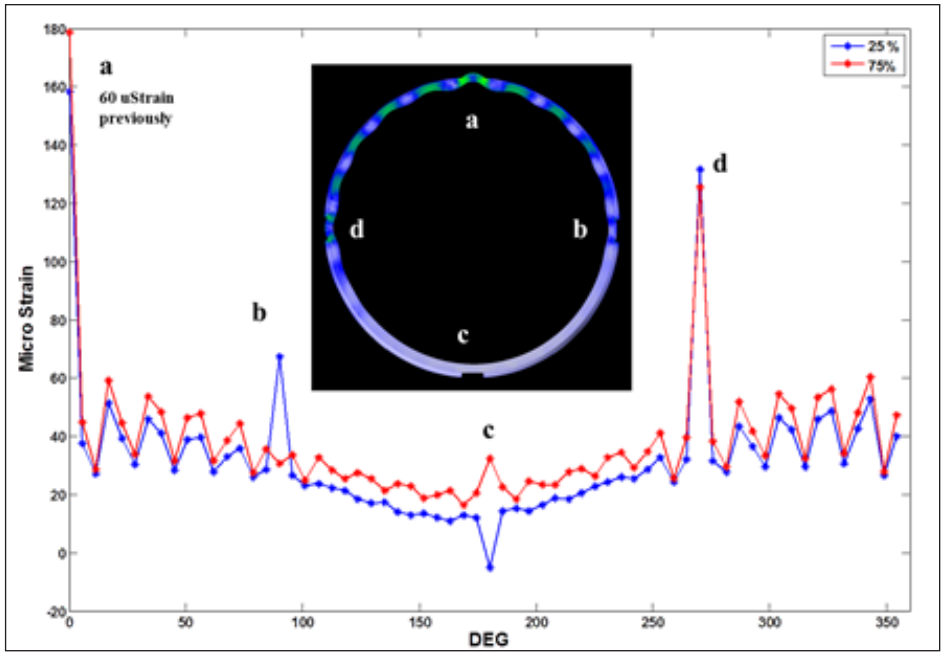

Figure 9 Modified outer raceway hoop strain of HS SH B for one-time step.

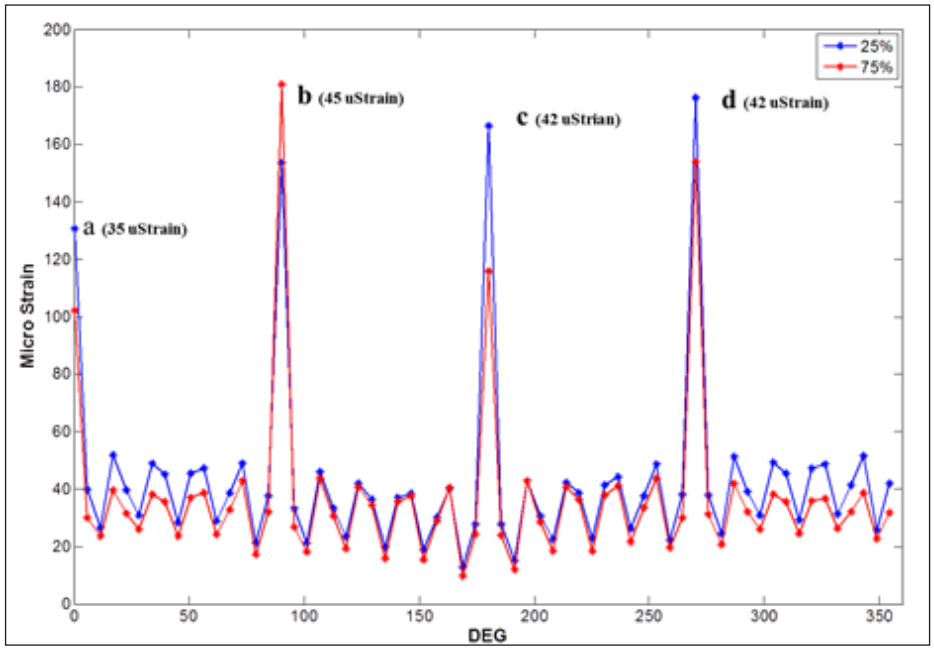

Figure 10 Modified outer raceway hoop strain of HS SH C for one-time step.

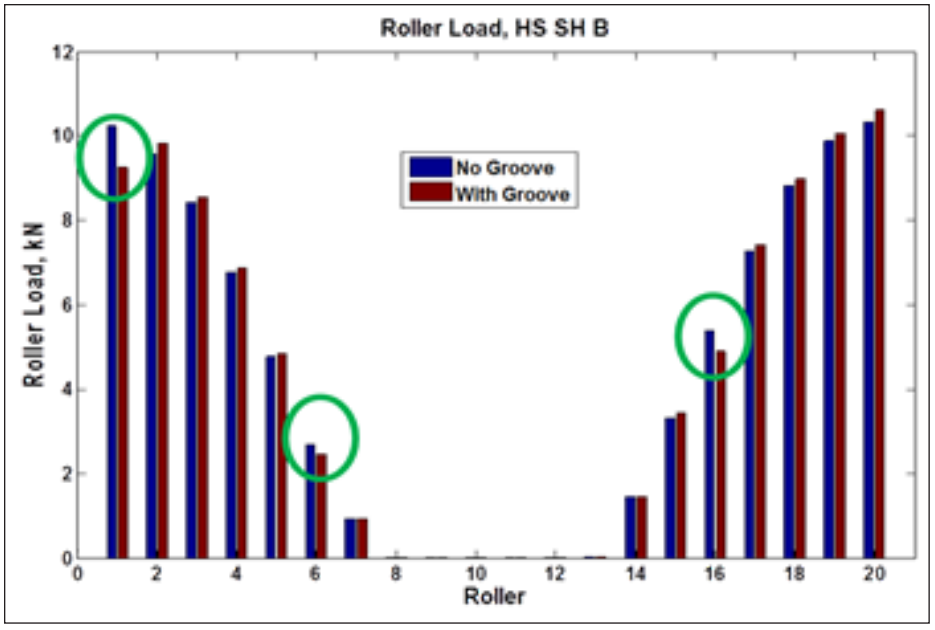

Figure 11 HS SH B roller loads — with and without modified raceway.

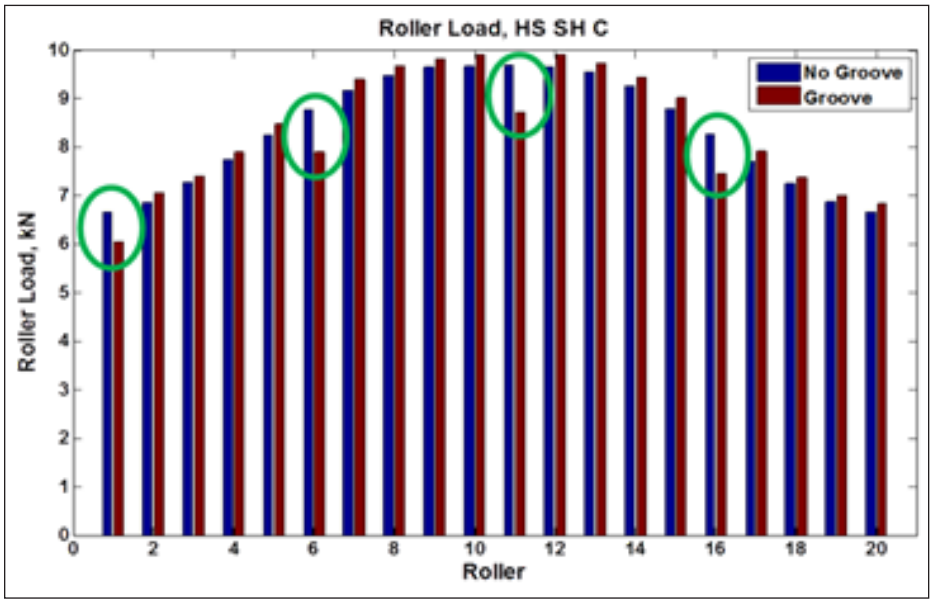

Figure 12 HS SH C roller loads — with and without modified raceway.

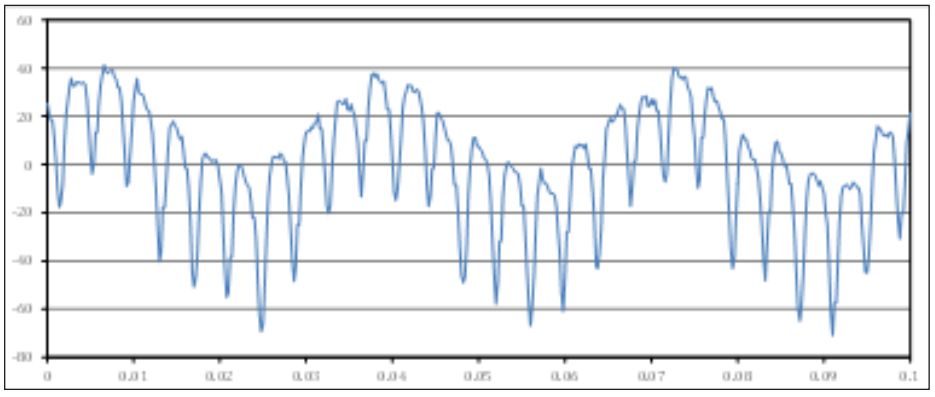

Figure 13 Measured modified outer raceway hoop strain in time for HS SH B, location "A" (0 deg), and axial position 75%.

HS SH C, respectively. Green-circled data points represent the locations of the outer raceway modifications; these figures show the total load carried by individual rollers for both the modified and unmodified outer raceway cases. Here the roller-to-roller load sharing is predicted to be minimally affected by the addition of compliance through the introduction of outer raceway grooves.

Implementation of Bearing Race Groove

The scheme discussed in this Section 2 has been implemented by the NREL Wind Energy group (Ref. 6) and successfully tested. Its final implementation has an adjusted groove geometry that was applied to accommodate manufacturing considerations. Also, the bearing preload that was achieved is unknown, but was most certainly considerably lower than that used in the example for this paper. To demonstrate the fidelity of the signals, Figures 13 and 14 show 0-degree slot strains for HS SH B and HS SH C at 75% axial location, respectively.

Strain caused by the direct application of load by a roller on the outer raceway is represented in Table 2 as the average peak-to-peak-measured strain. As seen in Figure 13, there is quite a bit of variability in strain levels for each different roller passing. This variability is quite repeatable, with roughly every ninth roller passing corresponding to one shaft revolution.

It should be noted here that a torque trace taken from the shaft showed a significant once-per-revolution torque variation that seems to correlate well with the strain variations.

Table 2 shows that HS SH B carries a small amount of load in comparison to HS SH C. As noted earlier — and predicted in Section 2 — this is due to the fact that the axial gear mesh load is supported by HS SH C, while the preload of HS SH B is reduced by this loading. In fact, for the 75% axial position of bearing HS SH B, it appears that virtually no load is carried by this end of the roller at positions C and D (Table 2). Because the analysis presented in Section 2 was performed assuming preload on this set of bearings, the simulations indicate more load carried by each of the bearings.

Conclusion

Here a full transmission model of a 750 kW wind turbine gearbox was modified in order to assess bearing raceway modifications for measurement of strain in order to predict bearing load sharing and load distribution.

It is clearly apparent that the modification of the tapered roller bearing outer raceways — through the introduction of a groove — greatly increased the predicted strain in the raceway.

Simulations predicted that appreciable strain signals could be produced by introducing such grooves, and measurements show that to be true.

Improved strain predictions to be directly compared to the experiments may be attained by using exact groove geometries manufactured, as well as the known, bearing preload levels used in the experiments.

Acknowledgments. *This work was partially funded by a grant (GRT0023734/60030753) from the National Renewable Energy Laboratory (NREL). We would like to thank Jon Keller and Yi Guo of NREL for providing us with the test data, as well as the sponsors of the Gear and Power Transmission Research Laboratory for providing funding for this research.* **PTE**

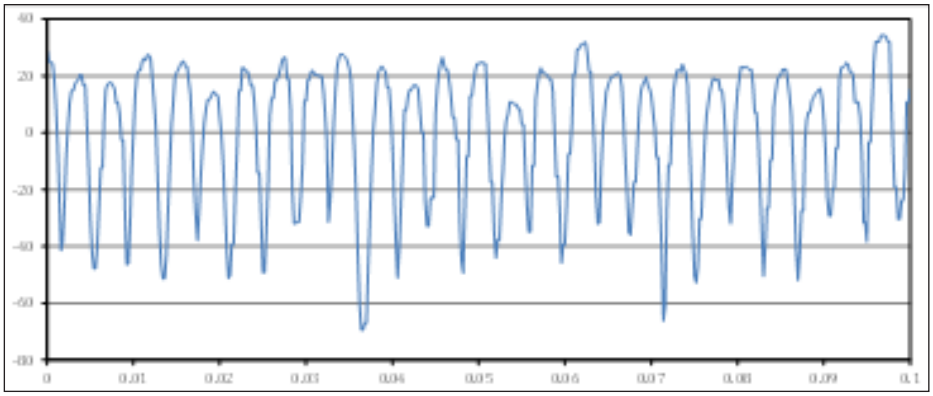

Figure 14 Measured modified outer raceway hoop strain in time for HS SH C, location "A" (0 deg), and axial position 75%.

Table 2 Measured peak-to-peak strains at groove locations with the modified bearing race.

Location	HS SH B (micro-strain) With Groove		HS SH C (micro-strain) With Groove	
	25%	75%	25%	75%
A	47	36	74	73
B	11	15	62	43
C	12	1	74	98
D	6	1	74	65

References

1. Musial, W. and S. Butterfield. "Improving Wind Turbine Gearbox Reliability," *Conference Paper NREL/CP-500-41548,* pp. 1-3, 2007.
2. Errichello, R. and J. Muller. "Gearbox Reliability Collaborative: Gearbox 1 Failure Analysis Report," *Technical Report NREL / SR-5000-53062,* 2012.
3. Wilson, R., S. Walker and P. Heh. "Technical and User's Manual for the *FAST_AD Advanced Dynamics Code*," *OSU/NREL Report 99-01*, Oregon State University, Corvallis, Oregon, 1999.
4. "*Transmission 3D* User's Manual," *Advanced Numerical Solutions, LLC, www.ansol.us*, 2014.
5. Vijayakar, S. "A Combined Surface Integral and Finite Element Solution for a Three-Dimensional Contact Problem," *Int. J. Numer. Methods Eng.*, 31 (3), 525–545, 1991.
6. Keller, J., Y. Guo and B. McNiff. "Gearbox Reliability Collaborative: High-Speed Shaft Tapered Roller Bearing Calibration," *Technical Report NREL/TP-5000-60319*, Oct. 2013.

Jason Austin graduated from the GearLab at Ohio State University in June, 2013, with an M.S in mechanical engineering. While there he authored a doctoral thesis on the FEA of a wind turbine gearbox via collaboration with the National Renewable Energy Laboratory and the Gearbox Reliability Collaborative. Austin is currently employed by DNV GL as a pipeline integrity engineer, tasked with providing technical consultation to the oil and gas industry.

David Talbot is a research scientist — mechanical and aerospace engineering — at The Ohio State University, specializing in gear system efficiency, manufacturing and geometry, and load distribution simulation.

Dr. Sandeep Vijayakar is founder and president of Advanced Numerical Solutions (ANSOL). He received his PhD from The Ohio State University, where he now serves as an adjunct faculty member. His company — ANSOL — specializes in the finite element contact analysis of gears. Vijayakar is credited with authoring the Calyx computer program, designed for the static and dynamic analysis of geared systems.

Dr. Donald Houser is Professor Emeritus of Mechanical Engineering and founder of the Gear Dynamics and Gear Noise Research Laboratory (GearLab) at Ohio State University. Dedicating his efforts and knowledge to gear dynamics research for over 45 years, he has also consulted for numerous companies. Dr. Houser is a past chairman of ASME's Power Transmission & Gearing, and Gear Noise Committees; is an active member of the AGMA Noise Committee; and has contributed gear noise-related chapters to *The Gear Handbook* (D. Townsend, editor) and *Handbook of Noise and Vibration Control* (M. Crocker, editor). Dr. Houser is also a prolific author of technical papers — presented at conferences and other proceedings worldwide — of which many have appeared in this publication.